Available online at www.sciencedirect.com
ScienceDirect
Journal of Power Sources 160 (2006) 711–715
JOURNAL OF POWER SOURCES
www.elsevier.com/locate/jpowsour

Efficient photocurrent generation through a self-assembled monolayer of C_{60}-mercaptophenylanthrylacetylene

Mun-Sik Kang, Seok Ho Kang, Hong Ma, Kyoung-Soo Kim, Alex K.-Y. Jen *

Department of Materials Science and Engineering, University of Washington, Seattle, WA 98195-2120, USA

Received 26 November 2005; received in revised form 26 January 2006; accepted 30 January 2006
Available online 29 March 2006

Abstract

A novel conjugated molecule, C_{60}-mercaptophenylanthrylacetylene (C_{60}-MPAA) has been self-assembled on a gold surface to form a highly ordered monolayer. The electrochemical properties of this molecule in solution or in a self-assembled monolayer (SAM) were investigated using cyclic voltammetry. A stable cathodic photocurrent was observed from a photoelectrochemical cell using the C_{60}-MPAA SAM modified gold as the working electrode in the presence of methyl viologen (MV^{2+}) as electron carrier. The quantum yield (14%) of the cell was obtained at a bias of −100 mV versus Ag/AgCl under the illumination of monochromatic light at 400 nm. The dependence of photocurrent on the potential bias applied to the self-assembled monolayer modified Au electrode indicated that electron flow from C_{60}-MPAA to the counter electrode through the electron carriers.

Keywords: Photocurrent generation; Quantum yield; Self-assembled monolayer; Electrochemistry; C_{60}

1. Introduction

Fullerene (C_{60}) is of great interest due to its unique electronic, spectroscopic and nanoscale physical structure [1–3]. Recently, C_{60}-derived self-assembled monolayers (SAMs) have been reported to exhibit a wide range of interesting properties such as charge transport, photo-conductivity, superconductivity, and biological activities [1–7]. Because of its electron-affinitive nature, it is possible to induce very efficient electron transfer from various photoexcited electron donors to C_{60} [4]. C_{60}s covalently bounded to conjugated molecules have been reported to form a long-lived charge-separated state via photoinduced electron transfer [8–11]. Therefore, various attempts have been made to develop photoelectrochemical cells with functionalized C_{60}s on electrodes [12–15] by taking advantage of the structural regularity of SAMs [16,17]. Although these results are very encouraging, there is a need to improve the order of these functional SAMs for enhancing their efficiency. In our earlier work, we have reported the observation of highly ordered self-assemblies from 4-mercaptophenylanthrylacetylene (MPAA) on Au(1 1 1) surface [18]. These molecules formed highly ordered two-dimensional arrays through an interplay of strong π–π intermolecular stacking and chemisorptive gold-thiol interactions. This stimulates us to synthesize a new hybrid molecule to combine the unique physical and electrochemical properties of C_{60} with the ordered self-assembly of MPAA SAMs to introduce interesting photoelectrochemical properties. In order to realize this, a new synthetic methodology has to be developed to covalently connect these two molecular moieties together. We have previously reported the synthesis of a novel functional hybrid molecule C_{60}-MPAA and its electronic behavior. Its SAM turned out to be stable and well-ordered on the gold substrate at room temperature [19]. Herein, we report electrochemical and photoelectrochemical properties of the C_{60}-MPAA self-assembled monolayer on gold.

2. Experimental

2.1. General methods

All commercially available reagents and solvents were used as received from commercial suppliers unless otherwise stated. Synthesis of MPAA and C_{60}-MPAA with acetyl (Ac) protection

* Corresponding author. Tel.: +1 206 543 2626; fax: +1 206 543 3100.
E-mail address: ajen@u.washington.edu (A.K.-Y. Jen).

0378-7753/$ – see front matter © 2006 Elsevier B.V. All rights reserved.
doi:10.1016/j.jpowsour.2006.01.082

is described elsewhere [18,19]. All the compounds were purified with column chromatography to analytically pure quality, and their chemical structures were fully confirmed by ^{1}H, ^{13}C NMR and mass spectroscopy.

2.2. Preparation of self-assembled monolayer on gold

The SAMs of MPAA and C_{60}-MPAA (Chart 1) were prepared by immersing Au(1 1 1)/mica substrates in toluene solutions containing 1.5 ml of either MPAA-Ac or C_{60}-MPAA-Ac at 25 °C for 48 h using 20 μl of ammonium hydroxide solution to deprotect the acetyl group. The concentration of each solution was same as 5×10^{-5} M. 0.4 ml of EtOH was added to increase the solubility of ammonium hydroxide. The thin film samples were rinsed with toluene and EtOH, and then dried with a stream of nitrogen.

2.3. Electrochemical and photoelectrochemical measurements

All electrochemical studies were performed on a Bioanalytical Systems, Inc. CV-50 W voltammetric analyzer using a three-electrode cell with a modified Au working electrode, platinum foil counter electrode, and a Ag/AgCl reference. Self-assembled monolayers on the gold were characterized to confirm the surface-confinement using cyclic voltammetry at scan rates ranging from 100 to 500 mV s^{-1} in the presence of tetrabutylammonium hexafluorophosphate (Bu_4NPF_6) dissolved in acetonitrile. Photoelectrochemical measurements were carried out in a one-compartment cell. The working electrode was illuminated with monochromatic excitation light of a certain wavelength through monochromator in 0.1 mM Na_2SO_4 aqueous solution containing 50 mM MV^{2+} as an electron carrier. The light intensity was monitored by a Multi-Function Optical Meter (Newport, Model 2835-C).

Quantum yield was calculated based on the number of photons absorbed by the C_{60}-MPAA on the gold at each monochromatic wavelength using input light intensity (0.85 mW cm^{-2}). Due to the low absorbance the absorption spectra of C_{60}-MPAA on gold could not be obtained. Therefore, the UV/vis spectrum of C_{60}-MPAA dissolved in toluene with known concentration was measured, and the molar extinction coefficient was calculated, under an assumption that the absorbance of the SAM is the same as that in solution [20,21]. The absorbance of C_{60}-MPAA on the gold was then calculated from the molar extinction coefficient and the surface coverage of C_{60}-MPAA on the gold obtained from electrochemical data.

3. Results and discussion

Cyclic voltammetry (CV) was employed to confirm the formation of SAMs on the gold. CV experiments of C_{60}-MPAA and its SAM on gold were carried out in acetonitrile containing 0.1 M of Bu_4NPF_6 as a supporting electrolyte at a sweep rate of 100 mV s^{-1}. Both the CVs of C_{60}-MPAA in solution and its assembly on Au have shown two electrochemically accessible and stable reduction states of C_{60} as shown in Fig. 1. The C_{60}-MPAA molecule exhibits two well-resolved reversible redox waves, at $E_{1/2} = -0.56$ and -0.95 V versus Ag/AgCl. These values are typical for those of the mono-functionalized C_{60} [20,22,23]. The first and the second peaks are attributed to the successive one-electron reduction of the C_{60} moiety. The CV results from the C_{60}-MPAA/Au SAM also reveal well-defined redox waves, $E_{1/2} = -0.57$ and -0.98 V versus Ag/AgCl. It indicates that the molecules are strongly adsorbed on the gold surface. Although the half-potential for the first and second

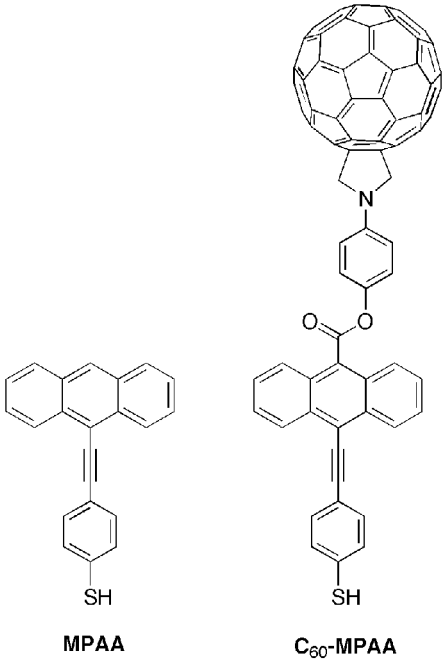

Chart 1. Chemical structures of MPAA and C_{60}-MPAA.

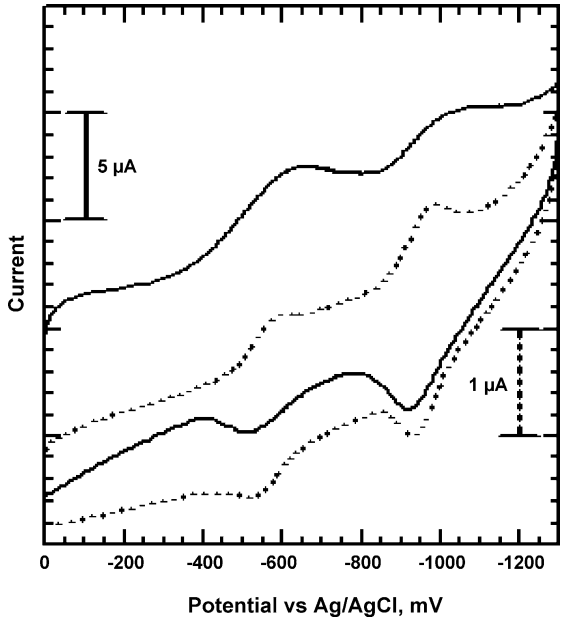

Fig. 1. Cyclic voltammograms of C_{60}-MPAA (dotted line) and its SAM on gold (solid line) were carried out in acetonitrile containing 0.1 M of Bu_4NPF_6 as a supporting electrolyte at a sweep rate of 100 mV s^{-1}.

reductions of the film have shifted to negative potentials (peak potential shift = 0.01 and 0.03 V for the first and second peak, respectively) compared to those of the hybrid molecules in solution, it resembles the results of the previously reported C_{60} SAMs [20].

The value of the peak splitting of C_{60}-MPAA/Au SAM ($\Delta E_{peak} = 115$ mV) is slightly larger than that of C_{60}-MPAA itself. This indicates slower redox kinetics between the C_{60} and the gold electrode because of the structural constraint on the substrate. However, the value of peak splitting is much smaller than the reported result ($\Delta E_{peak} = 180$ mV) using alkyl chain as a linker between gold electrode and C_{60} moiety [20]. It is noteworthy to mention that MPAA molecule is more effective for electron transfer between gold electrode and C_{60} moiety via π-conjugation than that by alkyl chains.

To confirm if C_{60}-MPAA/Au was surface-confined, cyclic voltammograms were carried out with different scan rate in the presence of 0.1 M Bu_4NPF_6 dissolved in acetonitrile. The results were shown in Fig. 2. As shown in Fig. 2 (inset), the cathodic peak current is linearly proportional to scan rate (over the range 100–500 mV s^{-1}) indicating that the molecules are surface-confined [24].

Integration of the area under the cathodic peak owing to the first reduction of C_{60} allows us to calculate the surface coverage of C_{60}-MPAA on the gold. The surface coverage of C_{60}-MPAA is 3.7×10^{-10} mol cm^{-2}. It is somewhat larger than the reported surface coverage using C_{60}. For example, the surface coverage is 1.9×10^{-10} mol cm^{-2} for a close packed monolayer of C_{60} [25] and 1.4×10^{-10} mol cm^{-2} for C_{60}-alkanethiol [21]. It is probably explained in two ways; first, actual surface area of gold is larger than geometrical area due to the surface roughness. The actual surface area is as high as 1.1 to 2.1 fold than geometrical area for the evaporated gold [26,27]. Second, the molecules of C_{60}-MPAA tend to pack well. As we reported earlier, high packing density is ascribed to the base molecule underneath C_{60} due to the π–π interactions [18,19].

In a separate report concerning the conducting behaviors of C_{60}-MPAA SAM, we have observed that it forms stable and highly ordered two-dimensional arrays at room temperature [19]. Taking advantage of these structural characteristics, we have investigated the efficiency of photocurrent generation in this hybrid system. The photo-electrochemical measurements of these SAMs were conducted in a Na_2SO_4 solution (0.1 M) containing 50 mM methyl viologen (MV^{2+}) as an electron carrier [28]. MPAA or C_{60}-MPAA SAM on gold electrode was used as the working electrode, and a platinum counter electrode and Ag/AgCl reference electrode were also used in the test configuration of Au/MPAA or C_{60}-MPAA SAM/MV^{2+}/Pt. The photocurrent was generated immediately when a monochromatic light source was used to illuminate the SAM of C_{60}-MPAA in electrolyte and the initial value of photocurrent went down instantly when the illumination was terminated. As shown in Fig. 3, photocurrent responses were recorded under the illumination of monochromatic wavelength of 400 nm with 0.85 mW cm^{-2} light intensity. When Au/C_{60}-MPAA /MV^{2+}/Pt was photo-irradiated under a bias voltage of −100 mV s^{-1} versus Ag/AgCl, a stable cathodic photocurrent (ca. 725 nA cm^{-2}) was generated, whereas MPAA on gold electrode showed very small photocurrent generation (less than 20 nA cm^{-2}) under the same illumination. It is revealed that C_{60} acts an excellent electron mediator between MPAA and MV^{2+} as well as a good electron acceptor. The amount of generated photocurrent of 725 nA cm^{-2} for Au/C_{60}-MPAA/MV^{2+}/Pt is comparable to the results reported by Imahori et al. using tripodal rigid anchor based on thiophene dye [29].

The action spectra of Au/C_{60}-MPAA /MV^{2+}/Pt roughly agree with the absorption spectra of molecule C_{60}-MPAA in solution (UV/vis spectrum in Fig. 4). It is believed that the MPAA

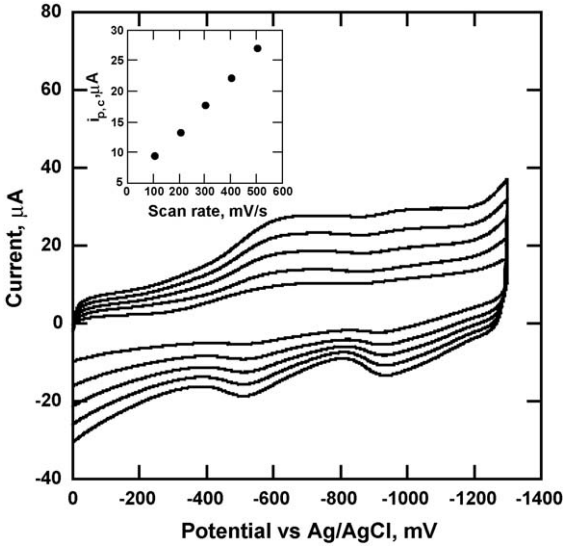

Fig. 2. Scan-rate dependence of the cyclic voltammograms of C_{60}-MPAA SAM on gold carried out in acetonitrile containing 0.1 M of Bu_4NPF_6 as a supporting electrolyte. The inset shows peak current as a function of scan rate.

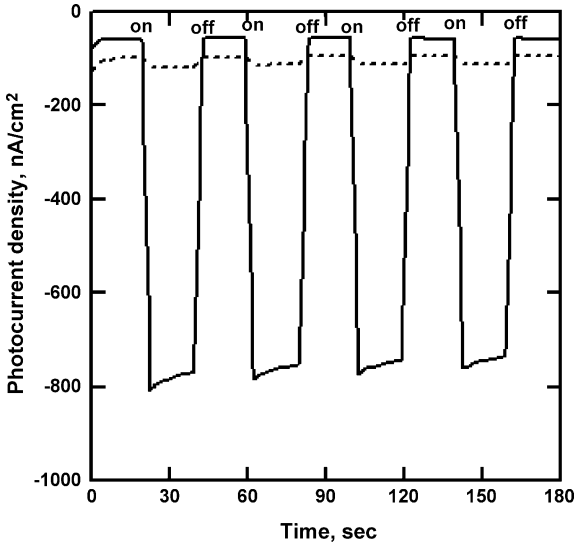

Fig. 3. Light-induced "ON"–"OFF" switchable photoelectrochemical response of MPAA SAM on the gold (dotted line) and C_{60}-MPAA SAM (solid line) on the gold: working electrode, Ag/AgCl (saturated KCl): Reference electrode, Pt: Counter electrode, electrolyte: 0.1 M Na_2SO_4 containing 50 mM methylviologen (MV^{2+}) with 0.85 mW cm^{-2} light intensity at −100 mV versus Ag/AgCl.

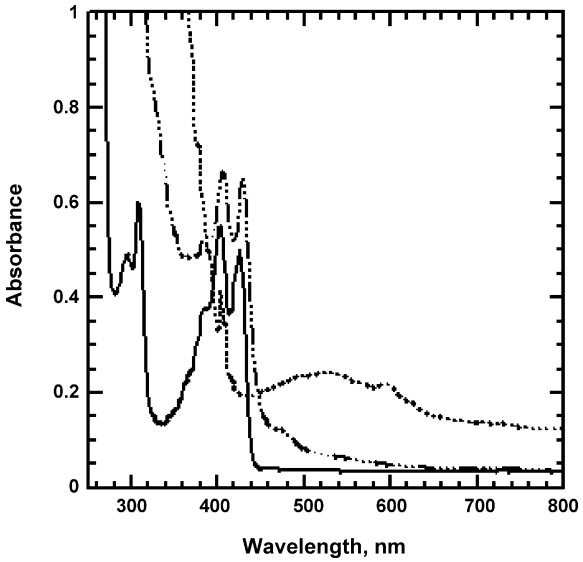

Fig. 4. UV/vis absorption spectra of MPAA (solid line), C_{60} (broken line) and C_{60}-MPAA (dotted line). The spectra are offset for the clarity.

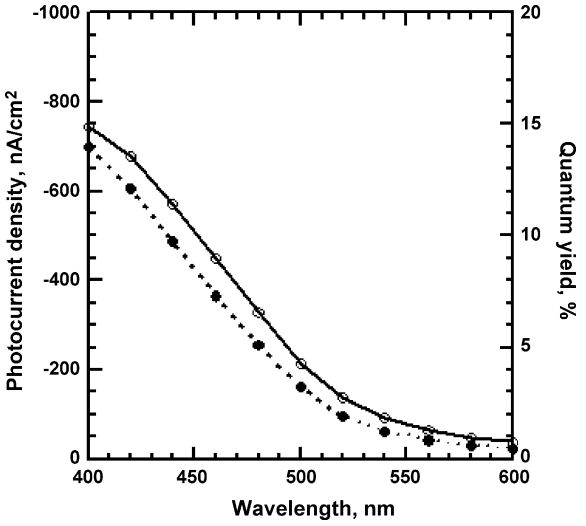

Fig. 5. Photocurrent action spectrum (solid line) of C_{60}-MPAA in the presence of 0.1 M Na_2SO_4 containing 50 mM methylviologen (MV^{2+}) with power intensity of 0.85 mW cm^{-2}. Effect of illumination wavelength on the quantum yields of the photocurrent (dotted line). The quantum yields were calculated using Eq. (1).

is a major photoactive species for the photocurrent generation at 400 nm. The difference of shape (no two bumps on action spectrum compared with spectrum in solution) between the two spectra may result from experimental error (we collected action spectra every 20 nm). Upon changing the excitation wavelengths within the range 400–600 nm, a photocurrent action spectrum were observed with a maximum at 400 nm, which is close to the absorption maximum in the range of investigated wavelength.

The quantum yields were determined in terms of the wavelength using photocurrent density, absorbance on the electrode and input power at the applied potential.

$$\Phi = \frac{i/e}{I(1-10^{-A})}, \quad I = \frac{W\lambda}{hc} \tag{1}$$

where i is the photocurrent density, e the elementary charge, I the number of photons per unit area and unit time, λ the wavelength of light irradiation, A the absorbance of the adsorbed dyes at λ nm, W the light power irradiated at nm, c the light velocity, and h the Planck constant [28]. As mentioned earlier, assuming that the absorption coefficient of C_{60}-MPAA on the gold is same as that in toluene ($\varepsilon = 2.2 \times 10^4\ M^{-1}\ cm^{-1}$ at 400 nm), absorbance of C_{60}-MPAA on the gold at 400 nm was calculated to be 8.5×10^{-3}. Based on the absorbance of C_{60}-MPAA on the gold, the quantum yield was determined. The quantum yield was increased with decreasing the wavelength as seen in Fig. 5. There is a good relationship between quantum yield and photocurrent generation at each wavelength. Fourteen percent of quantum yield was observed at −100 mV versus Ag/AgCl with a monochromatic wavelength of 400 nm. This value is larger than those in similar photoelectrochemical cells of porphyrin SAMs (0.1%) [30], C_{60}-linked alkane SAMs (7.5%) [20], and C_{60} LB cells (1.2–8.2%) [31].

To determine the direction of the current flow, the effect of bias voltage was investigated. Fig. 6 showed the photocurrent generated in this system, upon the application of different bias potentials on the electrode and the quantum yields in terms of the bias potential. The quantum yields were well matched with the photocurrent generation, that is to say, the quantum yields increased with increasing the photocurrent density at the potential range. The cathodic photocurrent dramatically increases when the bias potential passes +100 mV. However the attempt to increase the negative bias to more than –300 mV to the gold electrode could not be realized due to the significant increase of the cathodic current as the dark current. The semi-linear increase of the cathodic photocurrent in the presence of MV^{2+} with the increase of negative bias (from +200 to −200 mV versus Ag/AgCl) to the gold electrode under the illumination of 400 nm light demonstrates that the photocurrent flows from the gold electrode to the counter electrode

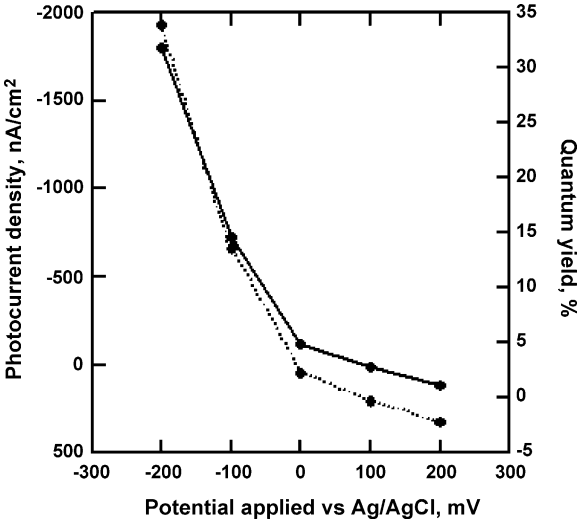

Fig. 6. Photocurrent density versus bias potential curves (solid line) for the C_{60}-MPAA SAM on the gold at monochromatic wavelength of 400 nm with 0.85 mW cm^{-2}. The quantum yields (dotted line) were shown as a function of the bias potential.

through the SAM and the electrolyte. This implies that the polarity of the electric field caused by the applied negative voltage is the same as the polarity of the inner electrical field (dipole moment of the SAM molecules) [32,33]. Based on the results together with UV/vis and the effect of bias voltage, the photocurrent generation mechanism can be considered as follows: the photoexcitation of MPAA chromophore induces electron transfer from MPAA to the covalently linked C_{60} moiety via intramolecular charge transfer, followed by electron transfer to the redox-species ($MV^{2+}/MV^{+\bullet}$) and then the electrons transfer from $MV^{+\bullet}$ to the counter electrode (Pt), thus resulting the observed cathodic photocurrent.

4. Conclusions

The electrochemical and photoelectrochemical properties of the gold electrode modified with C_{60}-MPAA have been studied systematically. The quantum yield (14%) of photocurrent generation of C_{60}-MPAA SAM on gold was obtained at −100 mV versus Ag/AgCl with a monochromatic wavelength of 400 nm. It reveals that the well-ordered SAMs of C_{60}-MPAA on the electrode is highly promising for the construction of efficient photocurrent generation.

Acknowledgements

Financial supports from the Air Force Office of Scientific Research (AFOSR) and Army Research Office (ARO-DURINT) are acknowledged. Alex K-Y. Jen thanks the Boeing-Johnson Foundation for its support.

References

[1] C.A. Mirkin, W.B. Caldwell, Tetrahedron 52 (1996) 5113–5130.
[2] H. Yamada, H. Imahori, Y. Nishimura, I. Yamazaki, T.K. Ahn, S.K. Kim, D. Kim, S. Fukuzumi, J. Am. Chem. Soc. 125 (2003) 9129–9139.
[3] Y.-J. Cho, H. Song, K. Lee, K. Kim, J. Kwak, S. Kim, J.T. Park, Chem. Commun. (2002) 2966–2967.
[4] W. Zhang, Y. Shi, L. Gan, C. Huang, H. Luo, D. Wu, N. Li, J. Phys. Chem. B 103 (1999) 675–681.
[5] G. Yu, J. Gao, J.C. Hummelen, F. Wudl, A.J. Heeger, Science 270 (1995) 1789.
[6] M. Prato, J. Mater. Chem. 7 (1997) 1097–1109.
[7] F. Diederich, M. Gómez-López, Chem. Soc. Rev. 28 (1999) 263–277.
[8] J.L. Segura, N. Martín, J. Mater. Chem. 10 (2000) 2403–2435.
[9] M. Fujitsuka, O. Ito, T. Yamashiro, Y. Aso, T. Otsubo, J. Phys. Chem. A 104 (2000) 4876–4881.
[10] P.A. Van Hal, J. Knol, B.M.W. Langeveld-Voss, S.C.J. Meskers, J.C. Hummelen, R.A.J. Janssen, J. Phys. Chem. A 104 (2000) 5974–5988.
[11] M. Fujitsuka, K. Matsumoto, O. Ito, T. Yamashiro, Y. Aso, T. Otsubo, Res. Chem. Intermed. 27 (2001) 73–88.
[12] H. Yamada, H. Imahori, Y. Nishimura, I. Yamazaki, T.K. Ahn, S.K. Kim, D. Kim, S. Fukuzumi, J. Am. Chem. Soc. 125 (2003) 9129.
[13] H. Yamada, H. Imahori, Y. Nishimura, I. Yamazaki, S. Fukuzumi, Adv. Mater. 14 (2002) 892.
[14] H. Imahori, H. Yamada, Y. Nishimura, I. Yamazaki, Y. Sakata, J. Phys. Chem. B 104 (2000) 2099.
[15] O. Dominguez, L. Echegoyen, F. Cunha, N. Tao, Langmuir 14 (1998) 821.
[16] A. Ulman, An Introduction to Ultrathin Organic Films, Academic Press, San Diego, 1991.
[17] A. Ulman, Chem. Rev. 96 (1996) 1533.
[18] M.H. Zareie, H. Ma, B.W. Reed, A.K.-Y. Jen, M. Sarikaya, Nano Lett. 3 (2003) 139–142.
[19] S.H. Kang, H. Ma, M.-S. Kang, K.-S. Kim, A.K.-Y. Jen, M.H. Zareie, M. Sarikaya, Angew. Chem. Int. Ed. Eng. 43 (2004) 1512–1516.
[20] H. Imahori, T. Azuma, A. Ajavakom, H. Norieda, H. Yamada, Y. Sakata, J. Phys. Chem. B 103 (1999) 7233–7237.
[21] S. Zhang, D. Dong, L. Gan, Z. Liu, C. Huang, New. J. Chem. 25 (2001) 606–610.
[22] L. Echegoyen, L.E. Echegoyen, Acc. Chem. Res. 31 (1998) 593–601.
[23] H. Imahori, T. Azuma, S. Ozawa, H. Yamada, K. Ushida, A. Aiavakom, H. Norieda, Y. Sakata, Chem. Comm. (1999) 557–558.
[24] X. Shi, W.B. Caldwell, K. Chen, C.A. Mirkin, J. Am. Chem. Soc. 116 (1994) 11598–11599.
[25] S. Liu, Y. Lu, M. Kappes, J.A. Ibers, Science 254 (1991) 408.
[26] D. Losic, J.G. Shapter, J.J. Gooding, Langmuir 17 (2001) 3307–3316.
[27] M.C. Leopold, E.F. Bowden, Langmuir 18 (2002) 2239–2245.
[28] H. Imahori, H. Norieda, H. Yamada, Y. Nishimura, I. Yamazaki, Y. Sakata, S. Fukuzumi, J. Am. Chem. Soc. 123 (2001) 100–110.
[29] D. Hirayama, K. Takimiya, Y. Aso, T. Otsubo, T. Hasobe, H. Yamada, H. Imahori, S. Fukuzumi, Y. Sakata, J. Am. Chem. Soc. 124 (2002) 532–533.
[30] H. Imahori, H. Norieda, S. Ozawa, K. Ushida, H. Yamada, T. Azuma, K. Tamaki, Y. Sakata, Langmuir 14 (1998) 5335–5338.
[31] C. Luo, C. Huang, L. Gan, D. Zhou, W. Xia, Q. Zhuang, Y. Zhao, Y. Huang, J. Phys. Chem. 100 (1996) 16685.
[32] W. Zhang, Y. Shi, L. Gan, N. Wu, C. Huang, D. Wu, Langmuir 15 (1999) 6921–6924.
[33] T. Morita, S. Kimura, S. Kobayashi, Y. Imanishi, J. Am. Chem. Soc. 122 (2000) 2850.